Journal of Global Engineering Research & Science (J-GERS)
Vol. 03, No. 02, December 2024, pp. 63-70
ISSN: 2830-5906, *e*-ISSN: 2830-5418, DOI: 10.56904/j-gers.v3i2.99

Optimizing Plastic Shredding Machine Blade Design Through ANSYS Simulation and Experimental Validation

Handi Satrio, Mohamad Zaenudin*
Department of Mechanical Engineering, Faculty of Engineering and Computer Science, Jakarta Global University, 16412, Indonesia

Article Info
Article history:
Received July 03, 2024
Revised August 29, 2024
Accepted September 04, 2024

Keywords:
Plastic recycling
Shredding machine
Cutting blade
Blade design
Stress analysis

ABSTRACT
Efficient plastic recycling depends on reliable size reduction. This study develops and evaluates cutting blades for a plastic shredding machine, integrating simulation, manufacturing, and performance testing. Finite-element analysis in ANSYS quantifies the effect of blade inner-radius on von Mises stress, equivalent strain, and tip deformation under operating loads. An intermediate inner-radius minimized stress concentration and deflection, indicating superior structural integrity. Manufacturing trials employed laser cutting; process parameters—cutting speed, lift height, nozzle standoff, and oxygen pressure—were tuned to minimize kerf defects and heat-affected zone, followed by finish grinding. The optimized blades delivered consistent comminution, yielding particles <30 mm with 62% size uniformity in shred tests. The results demonstrate that simultaneous optimization of geometry (inner-radius) and laser-cutting parameters enables durable, high-quality blades and improves downstream recycling efficiency. The study provides actionable guidance for blade design and fabrication and highlights the coupling between geometric stress control and manufacturability for sustainable plastic recycling systems.

Corresponding Author:
Mohamad Zaenudin
Department of Mechanical Engineering, Faculty of Engineering and Computer Science, Jakarta Global University, 16412, Indonesia
Email: mzaenudin@jgu.ac.id

1. INTRODUCTION

The utilization of plastic waste for recycling is crucial as part of efforts to combat the increasing accumulation of plastic waste. Plastic waste that remains in the environment without breaking down due to microorganisms can lead to a reduction in both organic and inorganic minerals in the soil. The development of plastic waste management systems must consider both environmental and operational aspects to ensure long-term viability [1]. One way to utilize plastic waste is through the recycling method. Recycling not only reduces the accumulation of waste in landfills and oceans but also conserves resources and energy [2]. In addition to conventional methods, innovative technologies such as pyrolysis are being assessed for their environmental footprint and integration into national waste management systems [3]. Other approaches, such as the valorization of non-recyclable plastics [4] and the adoption of blockchain-based tracking systems for recyclable materials [5], further enhance the efficiency and transparency of plastic waste handling. The Indonesian context, as explored by Damayanti et al. (2022) [6], reveals both the challenges and opportunities in modernizing plastic waste treatment infrastructure.

In the plastic recycling process, the initial stage involves shredding, which is carried out using a plastic shredding machine. This stage is critical as it converts used plastic into secondary raw materials in the form of flakes, facilitating further processing. The development of efficient plastic shredding technology is essential to improving the recycling of contaminated and heterogeneous polymer materials [7]. These smaller plastic flakes with uniform pieces serve as crucial feedstock in the subsequent recycling stages. The design and construction of effective shredding equipment are thus vital for supporting sustainable recycling systems. Plastic shredding machines generally consist of several main components: the machine frame, shredder blades, a plastic fragment

e-ISSN: 2830-5418, *p*-ISSN: 2830-5906

sieve, a protective top cover, and a drive motor. Enhancing the mechanical recycling stage, such as shredding, plays an important role in enabling plastic waste to be reintegrated into the production cycle with better efficiency and environmental performance [8]. Therefore, shredding not only supports the mechanical transformation of waste but also ensures the optimization of plastic waste management. Shredder-type plastic shredding machines are cost-effective and involve fewer manufacturing processes. The manufacturing process of plastic shredding machines includes selecting the right materials for the blades and machine structure, optimizing production techniques, and choosing efficient assembly methods. Additionally, cost considerations are crucial in the design and production of plastic shredding machines. In the effort to create effective and sustainable solutions, research is conducted to optimize cutting efficiency, blade wear resistance, and overall cutting blade production costs [9], [10].

The objective of this research is to enhance the performance of plastic shredding machines by improving blade design through simulation and experimental validation. Specifically, this study aims to identify the most efficient blade geometry using ANSYS Workbench simulations and validate the results through real cutting trials, with the goal of achieving a balance between performance, durability, and manufacturing cost.

2. METHOD

In this research, a shredder blade with two cutting edges and 5 various inner radius cutting edge simulation is used in a plastic shredding machine. The geometry and shape of the blade were designed using Ansys Workbench, and it includes a hexagonal hole to securely fit onto the drive shaft of shredder machine that couples to motors by V-belt. All dimensions and design specifications of the blade are illustrated in Figure 1. In this simulation, three variables are defined as follows. There will be three types of simulations conducted: stress analysis, strain analysis, and total deformation, which serve as the dependent variables for the product object. The independent variable is the plastic shredder blade of the single group cutter type, with variations in the inner radius of the cutting edge. The controlled variables include the material thickness, the overall diameter of the blade, and the support points on the shaft, all of which are kept constant [11]. The radius variations to be tested are R8, R10, R12, R14, and R16.

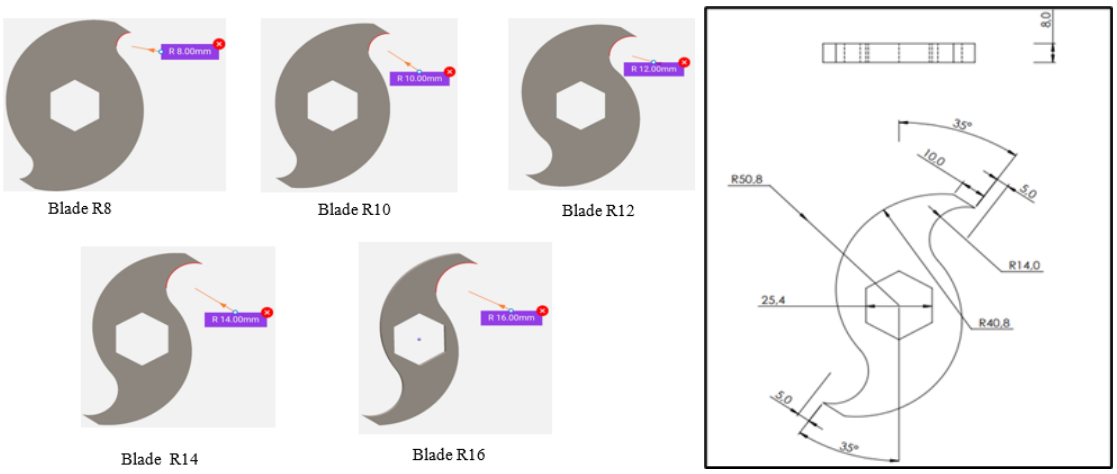

Figure 1. Variation of inner diameter geometry and detail dimensions

Based on the blade designs with variations in inner radius (R8, R10, R12, R14, and R16), a static structural analysis simulation was subsequently carried out using ANSYS software. The material used in the ANSYS simulation is AISI 1018, which is equivalent to commercially available mild steel or structural steel (SS400/ST37), The AISI 1018 material, with a tensile strength ranging from 370 to 440 MPa (average 405 MPa) and a yield strength between 250 and 310 MPa, is used to evaluate the durability of the shredder blade under operational loads. Its elastic modulus of 205 GPa affects the blade's deformation response to applied forces, while its hardness and impact strength contribute to resistance against wear and impact during use [4], detailed material properties is depicted in Table 1. These material properties form the basis for analyzing the blade's mechanical behavior through ANSYS simulation. A uniform cutting force of 240 N is applied to all blade variations. This force is calculated based on the minimum tensile strength of PET plastic (50–80 MPa), with a material thickness of 0.0025 mm and a blade cross-sectional area of 8 mm². The blade is fixed at the

center, and the force is applied at the cutting edge to simulate the shredding of plastic bottles, with the formula as follows:

$$\tau_{breaking\ plastic} = \text{safety factor} \times \text{tensile ultimate strength of PET}$$
$$\tau_{breaking\ plastic} = 1.5 \times 80\ \text{MPa}$$
$$\tau_{breaking\ plastic} = 120\ \text{MPa}$$
$$\tau_{breaking\ plastic} = 120\ \text{N/mm}^2$$

Table 1. AISI 1018 material properties.

Item	Value	Units	Notes
Material	AISI 1018	—	Used for the blade in ANSYS simulation; equivalent to mild steel/structural steel (SS400/ST37).
Tensile strength (range)	370–440	MPa	Average reported as 405 MPa.
Tensile strength (average)	405	MPa	Given explicitly.
Yield strength (range)	250–310	MPa	—
Elastic modulus	205	GPa	Governs elastic deformation response.

The blade has a thickness (w) of 8 mm (0.008 m), while the PET plastic being shredded has a thickness (t) of 0.000025 m. The cross-sectional area (A) of the plastic undergoing shredding is calculated using the formula $A=w\times t$, resulting in an area of 0.0000002 m². The cutting force (Fc) required for the shredding process was determined using the relationship between the material's shear strength and the cross-sectional area of the plastic being cut, expressed as $Fc=\tau\times A$. In this case, the shear strength (τ) of PET plastic was 120 MPa, while the cross-sectional area (A) was $2x10^5$ m². Substituting these values yields a cutting force of 240 N, which represents the theoretical force required to initiate the shredding process under ideal conditions. After selecting the supports or restraints, the next step is to define the meshing or element grid on the blade geometry. This process is carried out using the meshing algorithm in ANSYS Workbench, which divides the geometry into smaller elements, making it easier to perform finite element analysis (FEA).

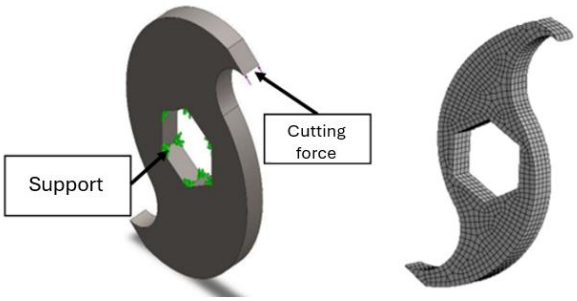

(a) (b)

Figure 2. (a) Setup (b) mesh

Figure 2 illustrates the setup used in a Finite Element Analysis to evaluate the structural response of a blade under shear and stress loading. The boundary conditions applied to the model, where a fixed support is assigned to the inner surface, constraining all degrees of freedom and simulating a rigid connection. A cutting force is applied at a specific location on the outer edge of blade. Figure 1b illustrates a meshed version of the model, indicating that the geometry has been discretized into finite elements to enable numerical simulation. To perform a mesh convergence test in ANSYS Workbench, several mesh sizes were tested to observe their influence on the simulation results, particularly the maximum von Mises stress. The mesh sizes evaluated were 5 mm, 3 mm, 2 mm, and 1 mm. Appropriate boundary conditions were applied, including fixed support and loading, and each mesh size was simulated independently. The resulting maximum stress values were 118.5 MPa for 5 mm, 119.0 MPa for 3 mm, 119.4 MPa for 2 mm, and 120.0 MPa for 1 mm mesh size. Using the result from the finest mesh (1 mm) as a reference, the relative errors were calculated for each case: 1.25% for 5 mm, 0.83% for 3 mm, and 0.50% for 2 mm. Based on these results, it can be concluded that mesh sizes of 2 mm and finer already provide acceptable accuracy, as their relative errors are below the standard convergence threshold of 1%. This indicates that the simulation has reached numerical convergence and that a 2 mm mesh offers a good balance between accuracy and computational efficiency This meshing process is a crucial step in FEA, as it influences the accuracy and convergence of the analysis results [12]. The combination of boundary conditions, applied loading, and mesh configuration enables the simulation to predict share, stress distribution, and deformation of the blade.

e-ISSN: 2830-5418, *p*-ISSN: 2830-5906

3. RESULTS AND DISCUSSION

Based on the simulation results, several parameters were evaluated, including total deformation, equivalent elastic strain, and equivalent stress. These parameters provide a comprehensive understanding of the blade's mechanical response under operational loads. Total deformation indicates the overall displacement experienced by the blade, while equivalent elastic strain reflects the recoverable deformation within the material's elastic limit. Equivalent stress helps assess whether the material is approaching its yield point, which is critical for preventing permanent damage or failure during operation.

3.1. Stress Analysis Result

Equivalent stress, also known as Von Mises stress, is a critical parameter used to describe effective stress within a material or structure, representing a combination of normal and shear stresses in three dimensions [13]. In the comparison presented in Figure 3.

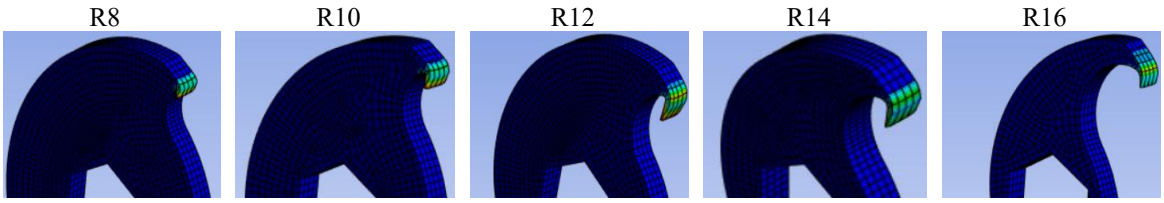

Figure 3. stress distribution pattern

Figure 3 shows each sub-image represents a stress distribution pattern on distinct blade geometries under an applied load, with the colored contours indicating varying levels of equivalent (Von Mises) stress. The red zones highlight areas of higher stress concentration, typically located near the cutting edge, suggesting the critical regions susceptible to wear or deformation during operation. This visual analysis aids in evaluating the mechanical performance and structural integrity of each blade configuration, providing insights into which design offers improved stress distribution and, consequently, better durability and cutting efficiency in plastic shredding applications

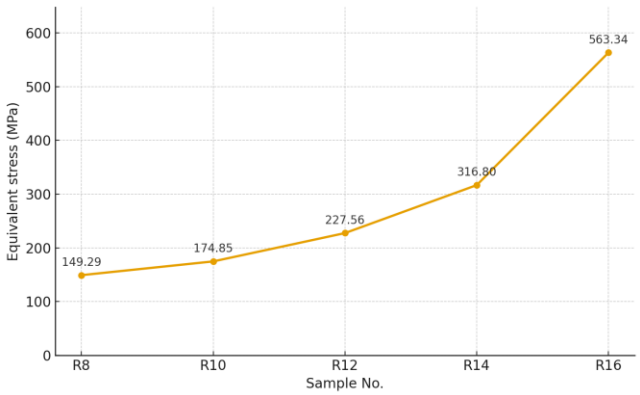

Figure 4. Equivalent (Von Mises) stress for each simulation.

Figure 4 presents the relationship between the blade tip radius (R8, R10, R12, R14, R16) and the resulting equivalent (von Mises) stress on the plastic shredder blade, based on simulation results using ANSYS Workbench. It can be observed that as the blade radius increases, the von Mises stress rises significantly. At R8, the stress is recorded at 149.29 MPa, while at R16 it reaches a maximum of 563.34 MPa. This increase indicates that larger blade tip radii lead to higher stress concentrations. This suggests that blade designs with larger radii are more likely to experience higher stress and may have a greater risk of structural failure. Therefore, selecting the optimal blade radius is essential to balance cutting efficiency and blade durability during the plastic shredding process.

3.2. Strain Analysis Result

Equivalent elastic strain is a parameter used to characterize the elastic deformation experienced by a material or structure. Elastic deformation occurs when a body undergoes a temporary change in shape that is fully recoverable upon the removal of the applied load [14]. The value of equivalent elastic strain indicates the

extent to which the blade undergoes elastic deformation at each tested radius. Higher values of equivalent elastic strain may suggest that the material is approaching its elastic limit, which could compromise performance if exceeded repeatedly. Monitoring this parameter is crucial to ensure that the blade operates within safe deformation limits under cyclic or repetitive loading. Furthermore, comparing strain values across different blade geometries helps identify optimal designs that maintain structural integrity while maximizing cutting performance.

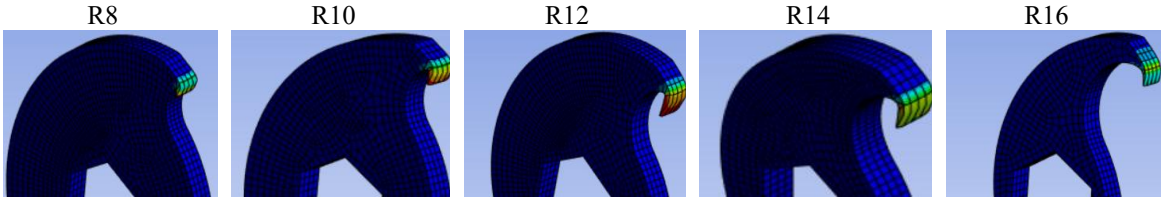

Figure 5. Strain distribution pattern

Figure 5 illustrates the strain distribution patterns obtained from finite element analysis of plastic shredder blades with varying tip radii (R8 to R16). As the tip radius increases, a notable change in strain behavior is observed under identical loading conditions. Blades with smaller radii (R8 to R12) exhibit localized and relatively moderate strain concentrations at the cutting edge, indicating effective stress distribution and limited deformation. In contrast, blades with larger radii (R14 and R16) show significantly higher strain intensity and broader distribution, particularly near the blade tip. This suggests that increased tip radius leads to elevated deformation and potential mechanical failure during operation. These findings highlight the importance of optimizing blade tip geometry to enhance the structural performance and durability of plastic shredding machines. Moreover, the FEA results serve as a predictive tool to minimize trial-and-errors in the design process, reducing material waste and manufacturing costs. Future design iterations can incorporate these insights to balance sharpness and structural resilience in blade development.

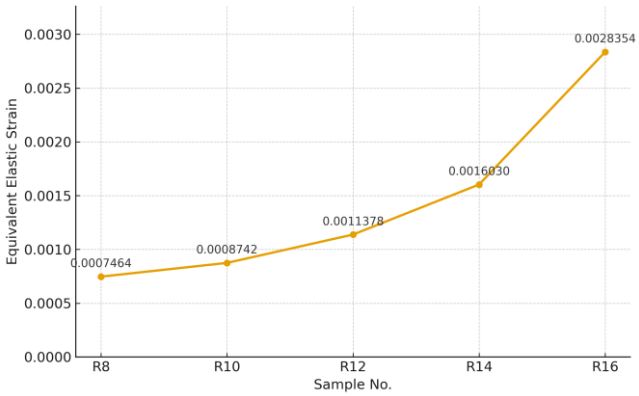

Figure 6. Equivalent elastic strain for each simulation.

The analysis of the graph in figure 6 indicates that the blade with an inner radius of R8 exhibits the lowest equivalent elastic strain value at 0.0007464 mm/mm. As the radius increases, there is a corresponding rise in strain, with R10 reaching 0.0008742 mm/mm, reflecting an increment of 0.0001278 mm/mm. The strain further increases to 0.0011378 mm/mm for R12, representing a 0.0002636 mm/mm rise from R10. R12 serves as the median among the five blade geometries. From R12 to R14, the equivalent elastic strain increases by 0.0004652 mm/mm, reaching a value of 0.0016030 mm/mm. The highest strain is observed in the R16 blade at 0.0028354 mm/mm, showing a significant increase of 0.0012324 mm/mm from R14. This trend clearly demonstrates that equivalent elastic strain increases progressively with larger blade radius. The most substantial rise occurs between R14 and R16, suggesting that blades with larger radii are subject to greater elastic deformation. This increased strain may offer enhanced flexibility during cutting operations, which could influence both the performance and durability of the blade. However, it is important to emphasize that these findings are derived from simulation data. Other contributing factors such as blade geometry, material composition, and loading conditions may also affect elastic strain behavior. Therefore, while these results provide valuable insights, further experimental validation is recommended to fully understand their implications in practical applications.

e-ISSN: 2830-5418, *p*-ISSN: 2830-5906

3.3. Total Deformation Analysis Result

Total deformation refers to the overall change in shape or size of a material or structure due to applied loads. For the cutting blade, the total deformation value indicates the extent of dimensional changes or deformation that occur during the cutting process or while operating the plastic shredding machine. Excessive deformation can lead to reduced cutting precision, increased wear, and potential misalignment with other machine components. Therefore, minimizing total deformation is essential to maintain cutting efficiency, ensure product consistency, and extend the blade's service life.

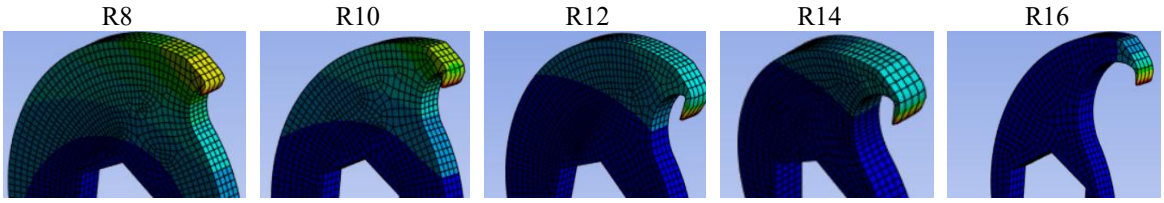

Figure 7. total deformation pattern

Figure 7 illustrates the total deformation distribution in five different blade designs with varying tip radii (R8 to R16) analyzed using finite element simulation. The deformation appears most pronounced at the cutting edge, particularly for blades with smaller tip radii, such as R8 and R10. As the radius increases, the deformation intensity at the blade tip decreases significantly. This trend indicates that larger tip radii contribute to a more uniform stress distribution and enhanced structural stability during operation. The results suggest that blades with smaller radii are more prone to higher deformation due to increased stress concentration, whereas blades with larger radii distribute the loads more effectively, reducing localized deformation. This analysis highlights the importance of tip radius optimization in achieving a balance between cutting performance and mechanical durability in plastic shredding blade design

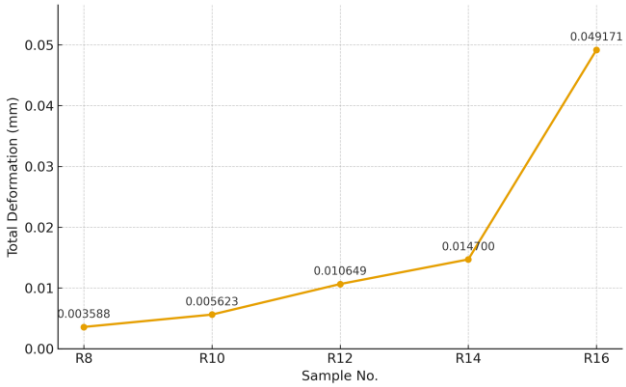

Figure 8. Total deformation for each simulation.

Figure 8 shows the total deformation increases with the blade radius. The smallest deformation, 0.003588 mm, takes place at R8, while R10 exhibits 0.005623 mm, R12 has 0.010649 mm, and R14 reaches 0.014700 mm. The largest deformation, 0.049171 mm, takes place at R16, with the biggest increase of 0.034471 mm from R14. R12, with a median deformation, offers the best performance compared to R14 and R16. This trend indicates that larger radii result in higher total deformation during the cutting process, which can impact cutting accuracy and blade stability. These results are based on simulations, and other factors like material properties, load conditions, and operational factors should also be considered in real-world applications. The sharp increase in deformation from R14 to R16 suggests a nonlinear relationship between blade radius and structural rigidity. As the tip radius increases, the cross-sectional area near the cutting edge becomes less capable of resisting bending forces, leading to amplified displacement underload. This could reduce cutting precision and potentially cause premature tool wear or failure. Therefore, while increasing tip radius might reduce wear concentration, it must be carefully balanced with mechanical performance to avoid compromising structural integrity.

A blade with an inner radius of R12 provides a practical balance between strength and stiffness under the applied load of 240 N. The simulation gives a von Mises stress of 227.56 MPa, which sits below the yield strength range of AISI 1018 (250–310 MPa). In other words, the safety margin relative to yielding is about 10–

36%, depending on the exact yield value used. The corresponding equivalent elastic strain is 1.1378×10^{-3}, and the total deformation is 0.010649 mm, yielding an effective stiffness of roughly 2.3×10^{4} N/mm. These values place R12 near the middle of the tested designs: it limits displacement much better than R16 and avoids the sharp rise in deformation seen from R14 to R16, while only modestly increasing stress compared with R10. Taken together, the results indicate that R12 controls deflection adequately and keeps stress within the elastic range for light-to-moderate duty. For applications requiring a larger safety margin, R12 can be retained by modest changes—such as using a stronger steel or slightly thickening the section near the blade root—or the load can be reduced. If no material or geometric changes are allowed, R10 offers more stress headroom with only a small trade-off in deformation.

3.4. Cutting Result

In this paper, blade radius 12 is the middle simulation result made by laser cutting process then conduct tests to optimize the performance of a plastic shredding machine with variations of plastic bottles. The motor speed was set to 483 rpm, and the cutting speed was based on the time taken to shred PET plastic bottles. The tests involved shredding 10 bottles, comparing the blade's performance before (laser cutting only) and after (grinding to sharpen) the grinding process. The uniformity of the shredding and machine capacity were calculated using the formulas for uniformity and capacity.

Table 2. Cutting results of the blades with radius 12 mm (R12).

Condition of Blade	Weight Before Shredding (g)	Fine Shredding (≤ 30mm) (g)	Shredding Uniformity (%)	Time (s)	Capacity (kg/hour)
Laser Cutting Only	14.5	65	45%	205	2.55
With Grinding	14.5	95	62%	185	2.82

The data shows that after grinding, the weight of fine shreds increased to 95 grams (from 65 grams), and shredding uniformity improved from 45% to 62%. The time to process 10 bottles decreased from 205 seconds to 185 seconds, and the machine capacity increased from 2.55 kg/hour to 2.82 kg/hour. This indicates that grinding enhances shredding efficiency, increases shred quality, and improves machine capacity. These improvements suggest that the blade's cutting edge becomes more effective after grinding, allowing for cleaner and faster cuts. Consequently, this can reduce energy consumption and wear on mechanical components, extending the operational life of the shredding machine.

4. CONCLUSION

Drawing on simulation and cutting trials, we conclude that blade inner-radius strongly governs the mechanics and product quality of plastic shredding: increasing radius from R8 to R16 monotonically elevates equivalent stress, elastic strain, and total deformation, with the largest values at R16 (stress 563.34 MPa, strain 2.8354×10^{-3}, deformation 0.049171 mm) and the smallest at R8; by contrast, R12 offers a balanced response, limiting displacement while avoiding the sharp rise in deformation observed from R14 to R16. Practical tests further show the decisive role of edge condition: post-laser grinding increased fine-shred mass from 65 g to 95 g, improved size uniformity from 45% to 62%, and raised throughput from 2.55 to 2.82 $kg \cdot h^{-1}$, underscoring that geometry selection must be paired with proper sharpening to achieve stable, efficient cutting. Overall, R12 is a defensible choice for the studied load and material, combining acceptable structural response with good shredding performance. Future research should (i) extend the parametric space to blade thickness, rake/clearance angles, and edge radius; (ii) test alternative steels and heat treatments with wear/fatigue assessments; (iii) couple thermo-mechanical, frictional, and dynamic effects in simulation with high-speed experimental validation; (iv) benchmark across polymers (PET, HDPE, PP) and operating loads/speeds; and (v) pursue multi-objective optimization (e.g., DoE/ML and its kind) targeting stress, deformation, energy per kg, and particle-size uniformity.

ACKNOWLEDGEMENTS

The authors would like to thank Jakarta Global University for its support throughout this project.

REFERENCES

[1] S. Huang *et al.*, "Plastic Waste Management Strategies and Their Environmental Aspects: A Scientometric Analysis and Comprehensive Review," *Int. J. Environ. Res. Public Health*, vol. 19, no. 8, p. 4556, Apr. 2022, doi: 10.3390/ijerph19084556.

[2] R. Balu, N. K. Dutta, and N. Roy Choudhury, "Plastic Waste Upcycling: A Sustainable Solution for Waste Management, Product Development, and Circular Economy," *Polymers (Basel).*, vol. 14, no. 22, p. 4788, Nov. 2022, doi: 10.3390/polym14224788.

[3] M. B. Karlsson, L. Benedini, C. D. Jensen, A. Kamp, U. B. Henriksen, and T. P. Thomsen, "Climate footprint assessment of plastic waste pyrolysis and impacts on the Danish waste management system," *J. Environ. Manage.*, vol. 351, p. 119780, Feb. 2024, doi: 10.1016/j.jenvman.2023.119780.

[4] S. Gazzotti, B. De Felice, M. A. Ortenzi, and M. Parolini, "Approaches for Management and Valorization of Non-Homogeneous, Non-Recyclable Plastic Waste," *Int. J. Environ. Res. Public Health*, vol. 19, no. 16, p. 10088, Aug. 2022, doi: 10.3390/ijerph191610088.
[5] K. Bułkowska, M. Zielińska, and M. Bułkowski, "Blockchain-Based Management of Recyclable Plastic Waste," *Energies*, vol. 17, no. 12, p. 2937, Jun. 2024, doi: 10.3390/en17122937.
[6] D. Damayanti *et al.*, "Current Prospects for Plastic Waste Treatment," *Polymers (Basel).*, vol. 14, no. 15, p. 3133, Jul. 2022, doi: 10.3390/polym14153133.
[7] J. Flizikowski, W. Kruszelnicka, and M. Macko, "The Development of Efficient Contaminated Polymer Materials Shredding in Recycling Processes," *Polymers (Basel).*, vol. 13, no. 5, p. 713, Feb. 2021, doi: 10.3390/polym13050713.
[8] I. Vollmer *et al.*, "Beyond Mechanical Recycling: Giving New Life to Plastic Waste," *Angew. Chemie Int. Ed.*, vol. 59, no. 36, pp. 15402–15423, Sep. 2020, doi: 10.1002/anie.201915651.
[9] M. Nasr and K. Yehia, "Stress Analysis of a Shredder Blade for Cutting Waste Plastics," *J. Int. Soc. Sci. Eng.*, pp. 0–0, Dec. 2019, doi: 10.21608/jisse.2019.20292.1017.
[10] J. H. Wong, W. M. J. Karen, S. A. Bahrin, B. L. Chua, G. J. H. Melvin, and N. J. Siambun, "Wear Mechanisms and Performance of PET Shredder Blade with Various Geometries and Orientations," *Machines*, vol. 10, no. 9, p. 760, Sep. 2022, doi: 10.3390/machines10090760.
[11] C. Pedraza - Yepes, P.-R. Miguel Angel, and P.-M. Giovanny Jose, "Analysis by means of the finite element method of the blades of a PET shredder machine with variation of material and geometry," *Contemp. Eng. Sci.*, vol. 11, no. 83, pp. 4113–4120, 2018, doi: 10.12988/ces.2018.88370.
[12] L. Sabat and C. K. Kundu, "History of Finite Element Method: A Review," 2021, pp. 395–404. doi: 10.1007/978-981-15-4577-1_32.
[13] M. Asgari and M. A. Kouchakzadeh, "An equivalent von Mises stress and corresponding equivalent plastic strain for elastic–plastic ordinary peridynamics," *Meccanica*, vol. 54, no. 7, pp. 1001–1014, May 2019, doi: 10.1007/s11012-019-00975-8.
[14] W. Tillmann, A. Eilers, and T. Henning, "Vacuum brazing and heat treatment of NiTi shape memory alloys," *IOP Conf. Ser. Mater. Sci. Eng.*, vol. 1147, no. 1, p. 012025, May 2021, doi: 10.1088/1757-899X/1147/1/012025.